Direct cortical control of muscle activation in voluntary arm movements: a model

Emanuel Todorov

Gatsby Computational Neuroscience Unit, University College London, 17 Queen Square London WC1N 3 AR, UK
Correspondence should be directed to E.T. (emo@gatsby.ucl.ac.uk)

What neural activity in motor cortex represents and how it controls ongoing movement remain unclear. Suggestions that cortex generates low-level muscle control are discredited by correlations with higher-level parameters of hand movement, but no coherent alternative exists. I argue that the view of low-level control is in principle correct, and that seeming contradictions result from overlooking known properties of the motor periphery. Assuming direct motor cortical activation of muscle groups and taking into account the state dependence of muscle-force production and multi-joint mechanics, I show that cortical population output must correlate with hand kinematics in quantitative agreement with experimental observations. The model reinterprets the 'neural population vector' to afford unified control of posture, movement and force production.

Since electrical stimulation of a region of cortex was discovered to evoke movement a century ago, the debate about the 'level' of movement control exerted by primary motor cortex (MI) continued[1]. Its crucial role in the production of all voluntary arm movements is evidenced by the almost complete paralysis following MI lesions[2]. Studies in awake behaving monkeys seem to establish that the activity of most MI pyramidal tract neurons is directly related to the amount of force exerted[3]. Such an involvement in low-level muscle control is consistent with the dense projection from MI to the spinal cord[4] (often directly onto motor neurons), and with linkage of corticomotor neuronal firing with muscle activity, as revealed by spike-triggered averaging[5].

This view is challenged by the observation that the MI population encodes both the direction[6] and magnitude[7,8] of movement velocity—cells encoding force should fire in relation to acceleration, not velocity. Yet the same cells that encode hand velocity in movement tasks can also encode the forces exerted against external objects in both movement and isometric tasks[9,10]. To complicate matters further, MI firing was also correlated with arm position[11], acceleration[12], movement preparation[13], target position[14], distance to target[15], overall trajectory[16], muscle coactivation[17], serial order[18], visual target position[19] and joint configuration[20]. In addition, the nature of the MI encoding seemed to vary systematically within each trial—with instantaneous movement curvature[7] or time from movement onset[15].

This plethora of correlations, previously summarized by the statement, "... all types of neuron that were looked for were found, in nearly equal numbers"[13], casts serious doubt on a low-level muscle-control theory of MI. However, there is no proposed alternative that is satisfying and equally simple. At one extreme, we have descriptive regression models[15,21] implying that MI neurons control every movement parameter that correlates significantly with their firing. Although these models can fit the data well, they leave a crucial question unanswered, namely, how such a mixed signal can be useful for generating motor behavior. The problem is that most of the proposed movement parameters are related through the laws of physics, and therefore the spinal circuitry cannot control them independently even if it somehow managed to decode the mixed MI signal in real time. The other extreme is to question whether "movement parameters are recognizably coded in the activity of single neurons" in the first place[22]. It is argued that they are not and do not need to be, as all that matters is the population average of the descending projections[22]. However it should still be possible to understand the average population activity, if not the firing of individual neurons. Yet a number of the above observations made on the population level conflict with one another.

My model assumes that each pyramidal tract neuron contributes additively, either via direct projections onto motor neurons or indirectly through spinal interneurons, to the activation of a muscle group[5] (see Methods). Thus muscle activity (motor neuron firing) simply reflects the firing in MI. How can such a model explain the numerous correlations with endpoint kinematic parameters? The basic idea is the following: these correlations are puzzling only if one assumes that muscle activation is identical to endpoint force. But that assumption is incorrect—muscle force depends not only on activation, but also on muscle length and rate of change of length[23–25]. Thus, to produce a certain endpoint force, the MI output has to compensate for the muscle's state dependence (as well as effects of multijoint mechanics). This position-and velocity-dependent compensation (a kinematic signal) gives rise to a number of correlations between MI firing and endpoint kinematics, which, taken at face value, imply a much higher level of MI control than is necessary to explain them.

In contrast with descriptive models that merely fit the data, my model is mechanistic: it first postulates how MI activity causes motor behavior, and then explains the observed correlations as emergent properties of that causal flow. Note that mechanistic models are more commonly used to explain their outputs given

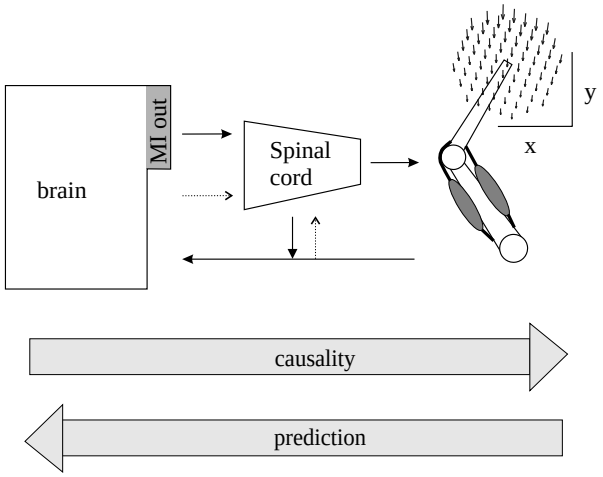

Fig. 1. Mechanistic model of the motor periphery. The 'brain' receives sensory feedback, combines it with motor plans, and somehow 'decides' what to do next. The focus of the model is the causal flow from the MI output through spinal processing, muscle force production and multijoint mechanics to endpoint force. Predictions about MI activity are obtained by 'inverting' that causal flow. Pathways corresponding to light arrows are ignored (but see Discussion). The illustrated position-dependent force field corresponds to an elbow flexor with fixed moment arm, acting around a planar 2-link arm with link lengths of 30 cm (not drawn to scale) over a 20 cm × 20 cm workspace. Note that direction varies little, and forces become smaller (because of muscle shortening) for displacements in the force direction. Such force fields will be modeled as parallel over the workspace of interest.

the inputs[26]. For a model of the motor periphery the situation is reversed (**Fig. 1**). The output (motor behavior) specified by the motor task is easily measured, and the input (MI firing) must be explained. This introduces a complication: the causal flow from MI firing to net endpoint force is a many-to-one mapping, and thus, is not invertible. Because there exists a large 'null-space' of MI firing patterns that all give rise to the same net force, the model cannot predict the activities of individual MI neurons. It can only predict that the observed MI firing will be constrained to the null-space corresponding to the observed endpoint force. This prediction takes the form of a population average, equivalent to the 'population vector' routinely computed in the experimental literature[6].

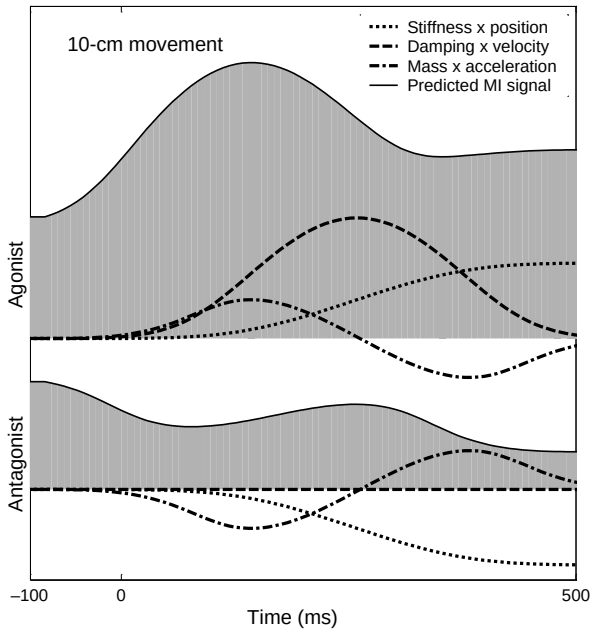

Results

Constraints on MI activity

I assume delayed linear summation of MI outputs, a first-order model of muscle force production, and a local linear approximation to multijoint kinematics over a small workspace. The impedance of the four-degree-of-freedom arm, muscle forces and movement kinematics are all expressed in two-dimensional endpoint space. The derivation in Methods yields the following result: the vector $\mathbf{c}(t-\Delta)$ of instantaneous MI outputs at time $t-\Delta$, multiplied by the matrix of a cell's endpoint-force directions, has to satisfy (up to an arbitrary scaling factor)

$$U\mathbf{c}(t-\Delta) = F^{-1}\mathbf{f}(t) + m\ddot{\mathbf{x}}(t) + b\dot{\mathbf{x}}(t) + k\mathbf{x}(t) \quad (1)$$

Average endpoint inertia, viscosity and damping are given by m, b and k, $\mathbf{x}(t)$is the two-dimensional hand position at time t, and $F_{2\times 2}$ is a matrix encoding the anisotropy of the Jacobian. (The Jacobian is the matrix of derivatives of endpoint coordinates with respect to joint angles.)

Equation 1 is the constraint mentioned above on the MI activation pattern $c(t-\Delta)$ corresponding to motor behavior $\mathbf{f}(t)$, $\ddot{\mathbf{x}}(t)$, $\dot{\mathbf{x}}(t)$, $\mathbf{x}(t)$. It is the starting point for all results presented below. Importantly, the activity of individual muscles was 'integrated out' (see Methods) so that the constraint on MI firing is expressed in endpoint space and depends only on behavioral parameters and arm impedance. The model has only four parameters—the scalars m, b and k and the aspect ratio of F—which all can be inferred from the literature (details in Methods and **Fig. 2**). Throughout the paper they are fixed to m = 1 kg, b = 10 N·s/m, k = 50 N/m, approximate values for the human arm. Scaling down all parameters does not affect the model.

To address experimental descriptions of individual cell firing, equation 1 is augmented with the assumption of cosine tuning[6] (and identical preferred directions) for force, velocity and displacement[9,11,27]. I show elsewhere that cosine tuning is the only activation profile that minimizes neuromotor noise—which makes it a principled choice. A sketch of that argument is given in Methods. Taking into account the asymmetry of muscle damping, the activation of cell c_i with force direction $\mathbf{u}_i$ is

$$c_i(t-\Delta) = C + \frac{\mathbf{u}_i^{\mathrm{T}}}{2}\left(F^{-1}\mathbf{f}(t) + m\ddot{\mathbf{x}}(t) + k\mathbf{x}(t)\right) + b\lfloor \mathbf{u}_i^{\mathrm{T}}\dot{\mathbf{x}}(t)\rfloor \quad (2)$$

Fig. 2. Composition of the MI signal, showing the signals for a 10-cm, 500-ms straight movement with a bell-shaped speed profile. The difference between agonist and antagonist activation is due to asymmetric damping, which is present only for muscle shortening (that is, in the agonist direction). Neural activity is advanced by Δ = 100 ms throughout the paper. In all simulations m = 1 kg, b = 10 N·s/m, k = 50 N/m. The terms m and b are proportional to perturbation estimates for the human arm[31], k is about 50% smaller for two reasons. Perturbation experiments measure combined effects of intrinsic muscle stiffness (which the model compensates for) and reflex contributions—in deafferented patients, stiffness is about 50% smaller[49]. More importantly, the slope of the isometric length-tension curve is much smaller than muscle stiffness measured via artificial, abrupt stretch[23] (presumably because of elasticity of crossbridges).

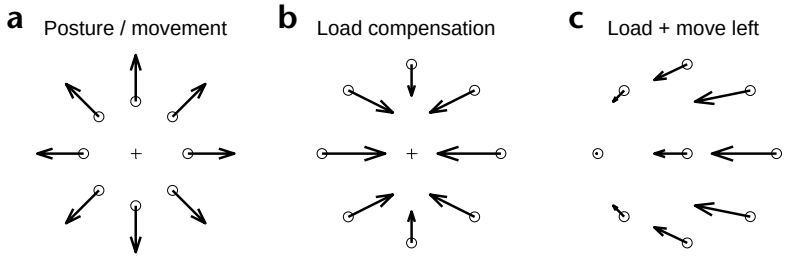

Fig. 3. Predicted population vectors. The origin (○) of each PV corresponds to the direction of movement/load relative to the center of the workspace (+). The movement PV is the average over the movement time: $\int_0^T (m\ddot{\mathbf{x}}(t) + b\dot{\mathbf{x}}(t) + k\mathbf{x}(t))dt$. The posture PV is the value at the end of the trial: $k\mathbf{x}(T)$. The load compensation PV is the value before movement: $F^{-1}\mathbf{f}(0)$. The combined movement + load PV is: $\int_0^T (F^{-1}\mathbf{f}(t) + m\ddot{\mathbf{x}}(t)\ b\dot{\mathbf{x}}(t) + k\mathbf{x}(t))dt$. The scale of the plots is arbitrary. The movement kinematics is given in Fig. 2. (**a**) The PV for movement/posture is symmetric. (**b**) Distortions of load PV result from the anisotropy of the F matrix (**f** opposes the external load and thus, the reversed direction). (**c**) Center movement to the left, no load. The eight surrounding clusters correspond to a movement to the left in the presence of three-newton loads in each of eight directions. The load magnitude is bigger than that used experimentally[9] because the impedance parameters here are also greater than those for a monkey arm.

It can be verified that the c_is given by equation 2 satisfy equation 1 under a uniform distribution of force directions. Note that $\mathbf{u}^T\mathbf{x}$ is the dot-product of vectors **u** and **x**, which is proportional to the cosine of the angle between them. The constant C can be thought of as a baseline or cocontraction command (specified independently).

Apparent velocity encoding

In the one-dimensional case, the quantity $U\mathbf{c}$ is simply the difference between agonist (A) and antagonist (N) activity: $c_A - c_N = f(t)/F + m\ddot{x}(t) + b\dot{x}(t) + kx(t)$. How is that quantity distributed between c_A and c_N? The simplest possibility is that it is divided equally, except for the asymmetric damping term which affects only muscles pulling in the direction of movement. Thus

$$\mathbf{c}_A(t-\Delta) = C + \frac{1}{2}(f(t)/F + m\ddot{x}(t) + kx(t)) + b\dot{x}(t)$$

$$\mathbf{c}_N(t-\Delta) = C - \frac{1}{2}(f(t)/F + m\ddot{x}(t) + kx(t)) \qquad (3)$$

During isometric force production, the only time-varying term is $f(t)$; thus the population seems to encode the magnitude of muscle force[3,5]. Now consider the activity of the same population during movement (**Fig. 2**). The crucial point is that, for hand kinematics in the physiological range with an experimentally measured inertia-to-damping ratio, the damping compensation signal actually dominates the acceleration signal. Thus the population activity resembles the velocity profile[7,8,27], although the cells directly control muscle activation. Note also the asymmetry between agonist and antagonist activity, which, in the model, is a natural consequence of muscle damping asymmetry. Although the latter effect is clear from several data sets[8,9,27], it is rarely commented upon.

Reinterpretation of the population vector

The lines of action of facilitated muscles overlap with the cell's physiological preferred direction (PD)[5]. To the extent that this also holds in the multijoint case, the neural population vector (PV), defined as the vector sum of PDs scaled by cell activations[6], is identical to the left-hand side of equation 1 ($U\mathbf{c} = \sum c_i\mathbf{u}_i$). In other words, the model predicts that the population vector, as commonly defined in the MI literature, is equal not to the movement direction or velocity[6,7], but instead to the particular sum of position, velocity, acceleration and force signals in equation 1. Additivity of movement and load-related signals is observed experimentally[9].

The predicted PV, the vector corresponding to the right-hand side of equation 1, for movement, posture, external-load compensation and movement with variable loads (**Fig. 3**) are in close agreement with existing data. The PV reconstructs the movement direction well[6,9], but the reconstruction of load direction is distorted[9], and the reconstruction fails when both movement and load direction are varied independently[28].

The difference between the movement and load compensation PV is interesting. The load compensation PV is significantly distorted—elongated for lateral directions and biased away from the center for diagonal directions. This in itself is not surprising, as unit endpoint forces in lateral directions require higher joint torques (and thus higher muscle activation) as a result of the Jacobian transformation. The question is, why is the same effect not present in the movement PV? In the model, this results from the interplay of the F, M, B

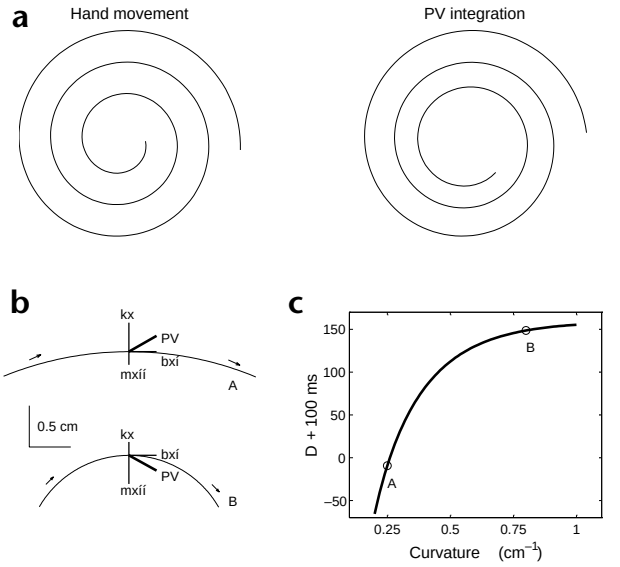

Fig. 4. Effects of curvature on PV direction. (**a**) Hand movement along a 1.5–7.5 cm spiral with a 2/3 power-law speed profile[7] and its reconstruction by integrating the predicted PV over time. (**b**) Interplay among the three signals for different curvatures—for small curvature, PV direction lags behind tangential velocity, while for large curvature it leads. (**c**) Consider movements along circles with different radii R (locally approximating a spiral), with angular velocities[7] well approximated by the 2/3 power law: $\omega = A\kappa^{2/3}$, where $\kappa = 1/R$ is curvature and $A \approx 12$ rad·cm per s. The hand trajectory is $x(t) = R\cos(\omega t)$, $y(t) = R\sin(\omega t)$. At $t = 0$ the tangent of the PV direction predicted by the model is $\frac{m\omega - k/\omega}{b}$ and the tangent of the instantaneous velocity is $\tan(\omega D)$. The solution $D = \text{atan}\left(\frac{m\omega - k/\omega}{b}\right)/\omega$ is plotted, offset by a constant delay of 100 ms from cortical firing to force production. The two marked points correspond to the examples in (**b**).

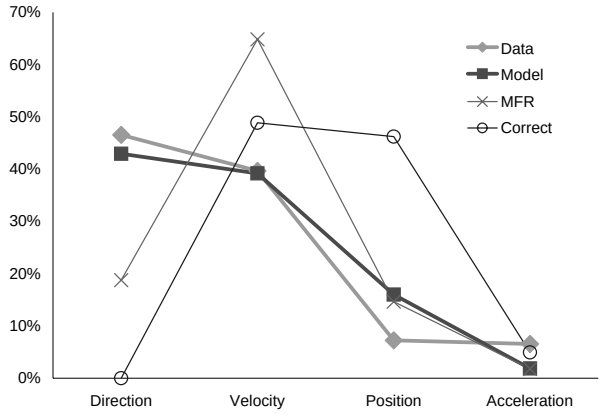

Fig. 5. Statistical biases in cell classification. The speed profile from Fig. 2 was scaled to match the hand kinematics shown in a previous study[21]. Movement extent, 0.15 m; peak velocity, 0.42 m per s; peak acceleration, 1.85 m per s^2. As previously[21], movement start and end were defined as the times when the hand left a central 10-mm circle and entered a 35-mm target circle, respectively. Time-varying mean firing rates were generated from the model for 290 cells[21]. Each cell had a random PD and its own parameters c_i, k_i, b_i and m_i generated independently between 0 and twice the corresponding average values of $c = 8.5$, $k = 50$, $b = 10$, $m = 1$. The profiles were multiplied by 2; this together with the baseline of $c = 8.5$ scaled the population activity between 5 Hz (anti PD) and 45 Hz (PD) as in a previous study[27]. Poisson spike trains were generated for five trials in each of eight directions with one-ms resolution and binned in ten-ms bins. The amount of smoothing (not given in ref. 21) was adjusted so that the median R^2 for the complete regression model matched the experimental value of 58%. The square root of the smoothed signal was defined as instantaneous activity[21]. For each cell, regressions of time-varying activity over all trials on direction, position, velocity and acceleration were performed separately, and the maximum R^2 was used to label the cell. The resulting percentages (model) are compared to experimental results[21] (data). The same procedure was repeated with the underlying mfrs instead of spike data. The 'correct' percentages were also computed by separately averaging for each cell the absolute values of the three signals over time and trials and then finding the maximum. Here, 20 sets of 290 cells were generated and the averaged results plotted. STDs for all data points were less than 3%; that is, 290 cells are sufficient to obtain robust estimates.

and K ellipsoids (see Methods). Because they are all elongated in the same (y) direction, their effects tend to cancel during movement. The proportionality assumption makes them cancel exactly, that is, the constants m, b and k are the same in all directions. Although exact values of these matrices for monkeys remain to be measured experimentally, their general shape is derived from the geometry of the multijoint arm.

The PV can be computed in small time bins at different points along the movement, and its direction compared to the direction of movement. If the PV encodes movement velocity it should always point along the movement, if it encodes force + acceleration, its direction should reverse in the decelerating phase of the movement. Here the PV is a combination of both, so reversals should occur when the velocity term becomes smaller than the force + acceleration term (that is, when moving faster or adding a mass to the hand). Indeed, such reversals are seen[29] in experiments in which a monkey moves while holding the end of a pendulum. These reversals become even more common as the mass of the pendulum is increased and do not occur during isometric force[10], in agreement with the model. Note that PV reversals are equivalent to the triphasic burst pattern (agonist–antagonist–agonist) described in EMG literature, which is most common during rapid movements. Thus I would predict an increase of PV reversals if monkeys were trained to move faster.

Interestingly, PV reversals are seen mainly during lateral movements, although arm inertia is larger in the forward direction. Why should that be the case? Recall that reversals arise from additional isotropic mass (m_1) which has the effect of adding $m_1 F^{-1}\ddot{\mathbf{x}}$ to the neural signal. Because F is elongated along the y axis, F^{-1} will be elongated along the x axis, thereby adding a larger force + acceleration signal in lateral directions.

Apparent fluctuations in MI-to-movement delay

Integrating the PV over time leads to a plausible reconstruction of hand paths[7]. Because the PV predicted by the model resembles movement velocity, integrating it leads to a similar reconstruction (**Fig. 4**). A more intriguing result suggests that the MI representation is time-varying, which would seem to contradict my model. Following this result, a time-varying delay $D(t)$ between MI firing and movement kinematics is defined in the following way: at each time step t, instantaneous PV direction is computed, and then the nearest time step $t + D(t)$ for which the direction of the tangential velocity is the same is found. The $D(t)$ computed in this way correlates with the curvature of the hand

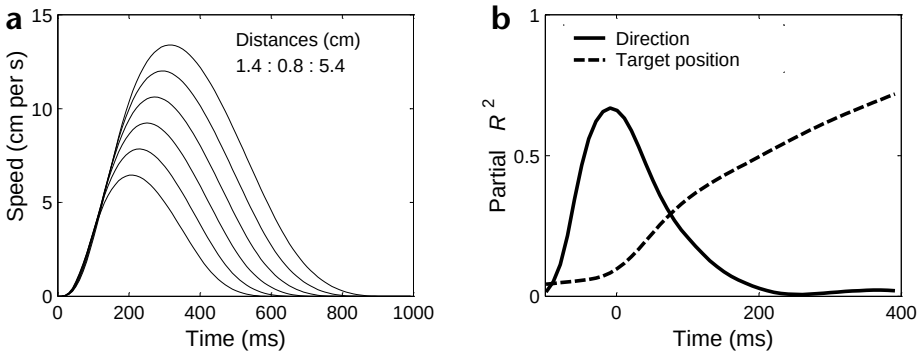

Fig. 6. Effects of kinematic scaling. (**a**) Skewed speed profiles in reaching at different distances, where peak velocity and movement duration scale with slopes 3 and 80 (in Hz, cm, ms) respectively[50]. (**b**) Simulation of 100 cells with uniformly distributed PDs, and time-varying mean firing rates (mfr) computed from the model, with ±1 Hz noise added in each 10-ms bin. Regression model at each time step t is: $\text{mfr} = a_0 + a_1 \cos\alpha + a_2 \sin\alpha + a_3 d \cos\alpha + a_4 d \sin\alpha$ where d is target distance and α is target direction. The partial R^2 between the mfr and 2D variable A is defined as the R^2 between A and the residual of the mfr regressed on B: $R^2_A = R^2(\text{mfr},A|B)$. A (B) are direction (target position) terms, and *vice versa*. Note that according to this definition, $R^2_{dir} + R^2_{pos} < R^2_{total}$ because of correlations between the target direction and position terms.

path[7], being greater for large curvature and smaller (even negative) for small curvature (which implies that MI does not control but, instead, responds to parts of the movement).

This behavior is also observed in the model. The apparent fluctuations in $D(t)$ result from incorrectly treating the PV as a pure velocity signal[7]. The explanation is that for large curvature, the acceleration vector pointing inwards is large, advancing the PV direction relative to tangential velocity (**Fig. 4**). For small curvature and large movement radius, the acceleration vector is smaller and the position vector larger—yielding the opposite effect. A more precise analysis (**Fig. 4**) accounts quantitatively for three important features of the experimental data: $D(t)$ increases with curvature, the $D(t)$ curve is very steep for small curvatures and saturates for larger curvatures, and $D(t)$ can actually become negative. Thus the curvature-dependent changes in the MI-to-movement delay are observed only when $D(t)$ is computed using the instantaneous hand velocity, rather than the signal I propose.

Apparent significance of velocity/force direction

The remaining analyses are based on the model of individual cell responses in equation 2. Particularly important here are demonstrations of a significant contribution of velocity and force direction irrespective of magnitude[21,30]. Such results would seem to contradict the model, which contains no explicit directional terms. The model successfully replicates those results, and clarifies what implicit assumptions and statistical biases cause the apparent contradiction.

For a center-out reaching task[21], time-varying mean firing rates of individual neurons are regressed on four different sets of two-dimensional predictor variables: target direction (constant in each trial), measured hand position, velocity and acceleration. For each cell, the four separate regression models were compared and the cell was classified according to the model with highest R^2 value. Target-direction cells were most common (47%), suggesting that target direction was the most prominent factor underlying MI activity. The small percentage (6%) of hand-acceleration cells was used to argue against force-control models in general.

Surprisingly, replication of this analysis in detail on synthetic data[21] (equation 2; **Fig. 5**) yields very similar results—target direction is again most prominent (43%), although the synthetic data is generated without any directional term. How is that possible? The first reason is a major statistical bias resulting from the smoothing of single-trial spike trains and taking the square root[21]. In the model, that step can be avoided by 'observing' the true mean firing rates instead of spike trains, and then applying identical analysis. That change is sufficient to decrease the percentage of target direction cells from 43% to 19%. But the direction cells still account for 19%, when a correct inference procedure should not find any. This is possible because the D, P, V and A waveforms used as predictor variables are correlated, and a linear combination of P, V and A can be more similar to D than any of its constituents. Thus, even with 'ideal' data, the prior assumption that direction cells exist is itself sufficient to bias the result of the analysis. Such biases raise the important question of how one can ever determine what an individual neuron controls[22].

A related result comes from a three-dimensional isometric force study[30] that contrasted the contributions of force magnitude M and unit-length force direction vector X, Y, Z. Two regression models of cell firing d were compared: (D) $d = b_0 + b_xX + b_yY + b_zZ$ and (M) $d = b_0 + b_mM$. Because only model (D) was significant in 79% of the tuned cells, it was concluded that force direction, and not magnitude, is the most important determinant of MI firing.

To test whether the model replicates the results of this three-dimensional study, a similar two-dimensional analysis was applied to 300-ms Poisson spike trains for 150 synthetic cells, with firing rates scaled between 5 Hz (anti PD) and 50 Hz (PD), on 192 trials with different static forces[30]. For roughly 90% of the synthetic cells only model (D) was significant at $p < 0.05$, and both models (D) and (M) were significant for the remaining 10% of cells. This is because the analysis implicitly assumes additive contributions of direction and magnitude: (D + M) $d = b_0 + b_xX + b_yY + b_mM$. But the correct regression model for the synthetic data is a multiplicative one: (DM) $d = b_0 + b_{xm}XM + b_{ym}YM$. Indeed, model (DM) had a higher R^2 value (by 10% on average) than model (D + M) for each of the 150 synthetic cells, although it used one less parameter. Thus the original result may be due to a specific assumption regarding combination of the force direction and magnitude in the MI firing[30], which is violated in my model.

Apparent signal multiplexing

Another intriguing result indicates a temporal multiplexing of different signals in the MI population activity[15], which would again seem to contradict the model. In a center-out reaching task with varying target direction (8) × distance (6), the strength of partial correlations between MI activity and target direction is higher around movement onset; later, partial correlation is higher with target position, and even later, with target distance[15]. The first two results can be explained by applying the model to the hand kinematics inferred from this study[15]. The key is the following: in reaching to more distant targets, both the peak velocity and movement duration scaled up, in agreement with the speed–accuracy tradeoff known as Fitt's law. As a result, the initial portions of the speed profile seem very similar across target distances (**Fig. 6**, left). Thus the MI encoding predicted by the model is best correlated with target direction around movement onset, and later becomes better correlated with target position (**Fig. 6**, right). An even later correlation with distance could be explained if cocontraction increased around the time of target acquisition[31] in proportion to movement velocity.

This analysis leads to an important general point: the relative contributions of different movement parameters to MI firing are not invariant physiological characteristics, but depend on the details of motor behavior. To avoid reaching different conclusions about MI's role whenever the monkey moves faster or holds an extra mass, the relative magnitudes of different kinematic and kinetic terms as observed in the task must be taken into account together, rather than normalized separately as they are in regression analyses.

Discussion

In summary, I formulated a simple mechanistic model of force production which incorporates known properties of muscle physiology and multijoint mechanics. The model accounts for six main results. First, force magnitude is encoded in isometric tasks and velocity seems to be encoded in movement tasks; second, velocity is not encoded near the anti-preferred direction; third, directional PV is asymmetrical in force-related results but not in movement-related results; fourth, velocity and force direction seem to dominate without respect to magnitude, fifth, changes in MI-to-movement delay seem to dependent on curvature, and sixth, direction and target position signals seem to be temporally multiplexed. At first glance, any one of these physiological find-

ings rules out earlier views of direct MI involvement in the control of muscle activation[3]. However, the contradictions can be traced to the incorrect implicit assumption that muscle activation alone determines endpoint force. In my model, most of these puzzling phenomena arise from the feedforward compensation of muscle viscoelasticity. Although realistic muscle properties are incorporated in one previous model of cortical control[32], such compensation is not considered. A previously proposed additive model[9] is related to equation 1, but all terms in it are interpreted as torque components—leaving the similarity to the velocity profile[8] unexplained.

My model by no means provides a complete picture of MI into which all known pieces can fit. It is only a first approximation that attempts to solve as many puzzles as possible while assuming as little as possible. Clearly, equations 1 and 2 can only hold when MI and muscles are simultaneously active. For instance, in instructed-delay tasks, some form of gating at the level of the spinal cord must be assumed to explain how MI neurons can be active long before muscle activation.

Perhaps the most debated of the issues left out is that of reference frames. Studies that vary workspace location[33] or arm posture[34] yield changes of MI encoding consistent with a joint or muscle-based representation[35], in agreement with the model. A similar experiment with wrist movements[36] gives more mixed results—changes in preferred direction are consistent with both extrinsic and muscle-like encoding in different subpopulations. However, unlike a truly 'extrinsic' cell, most of the 'extrinsic' cells change their overall firing rate with posture. Such gain changes can be sufficient to maintain the consistency of equation 1 (which in itself implies no similarity between responses of individual cells and muscles). In particular, consider a muscle m driven by two cosine-tuned cells with gains $a_{1,2}$ and preferred directions $\mathbf{p}_{1,2}$. Omitting baselines, the muscle activity for force direction $\mathbf{f}$ is $m = a_1\mathbf{f}^T\mathbf{p}_1 + a_2\mathbf{f}^T\mathbf{p}_2 = \mathbf{f}^T(a_1\mathbf{p}_1 + a_2\mathbf{p}_2)$, that is, the muscle is cosine-tuned with preferred direction $a_1\mathbf{p}_1 + a_2\mathbf{p}_2$. This vector can be rotated either by rotating $\mathbf{p}_{1,2}$ or by keeping $\mathbf{p}_{1,2}$ fixed and only varying $a_{1,2}$. To test whether this mechanism explains the results[36] would require knowledge of the 'muscle fields' of individual neurons, which could be recorded using spike-triggered EMG averaging[5].

In isometric force tasks, the descending MI population activity is more phasic than EMG activity[37]. This phenomenon may be entirely restricted to the onset of each trial, that is, an extra burst of activity may be required to overcome thresholds in the motor periphery. It is unlikely to encode an initial force transient[32], because such a force transient is absent in isometric tasks[37]. The few studies focusing on more prolonged behaviors fail to report any such effects in MI[7,17] or the red nucleus[38] (another source of descending projections). Furthermore, the model is concerned only with pyramidal tract neurons, whose activity is less phasic than that of a mixed MI population[9]. If this initial phasic activity is indeed a transient 'higher-order' correction that does not reflect the underlying mode of MI control, it is better to omit it from the model at this stage. If future experiments indicate that the MI output is always more phasic that EMG activity, that is, some form of low-pass filtering takes place in the spinal interneurons, the term $U\mathbf{c}(t-\Delta)$ in equation 1 may have to be replaced by Filter$(U\mathbf{c}(t-\Delta))$. The low-pass filtering present in muscles[24,25] can also be included. Then, to generate predictions about MI population activity, the right-hand side of equation 1 has to be unfiltered (deconvolved)—essentially adding terms proportional to its derivatives and making the prediction about $U\mathbf{c}(t-\Delta)$ more phasic.

The general model of central control deserves further discussion. It implicitly assumes that in the simple, overtrained, unperturbed movements studied here, feedforward central control can be quite accurate. Thus the limb will move very close to the reference point for activating spinal reflex loops, minimizing their contribution to muscle activity. This model assumption is similar to the conclusions of psychophysical studies[39], as well as robotic-control algorithms motivated by computational efficiency and manipulator stability[40]. If this assumption turns out to be incorrect and reflexes always contribute significantly to muscle activity, their gains could be added to the corresponding impedance terms in the present formulation. Similarly, descending projections from the red nucleus could be included in the vector $\mathbf{c}(t-\Delta)$—in agreement with experimental observations[38].

Methods

Notation. x is a scalar, $\mathbf{x}$ is a column vector and $\mathbf{x}^T$ is a transposed (row) vector. Thus $\mathbf{x}^T\mathbf{y}$ is the dot product of $\mathbf{x}$ and $\mathbf{y}$, X is a matrix, Diag $(\mathbf{x})$ is the diagonal matrix with vector $\mathbf{x}$ along the main diagonal, $\lfloor x \rfloor$ returns x for positive numbers and 0 otherwise, $\dot{\mathbf{x}}$ and $\ddot{\mathbf{x}}$ are temporal derivatives of $\mathbf{x}$, $|X|$ is a determinant, and X^{-1} is a matrix inverse.

Model formulation. The muscle activations a_i are modeled as time-delayed sums of MI pyramidal tract activities c_j multiplied by synaptic weights w_{ij}; in vector notation, $\mathbf{a}(t) = W\mathbf{c}(t-\Delta)$. A similar linear summation model captures the relationship between EMG and red nucleus activity[38]. Comparisons of onset time and activation magnitude between MI and EMG[41] support such a direct activation model. Also, the effects of simultaneous microstimulations add linearly—both in terms of endpoint force fields[42] and EMG activity[43].

The mechanisms of muscle force production have been well characterized, both on the microscopic and macroscopic levels[24,25]. For fixed activation a, muscle force f varies with length l and velocity $\dot{l}$ (l increases in the direction of shortening). The effect of velocity (damping) is asymmetric; it is predominantly present during shortening[23]. The first-order model $f(a,l,\dot{l}) = a - kl - \lfloor b\dot{l} \rfloor$ provides a reasonable approximation[25] (a is assumed large enough to prevent f from being negative).

The direction of hand movement for which a muscle shortens most rapidly is very close to the direction in which it produces endpoint force, and its orientation varies little over a small workspace (**Fig. 1**). Thus the position- and velocity-dependent endpoint-force field $f_i(a_i,\mathbf{x},\dot{\mathbf{x}})$ that muscle i generates can be summarized by a 'muscle force vector' $\mathbf{p}_i$ and the coefficients k_i, b_i:

$$\mathbf{f}_i = \mathbf{p}_i\,(a_i - b_i\lfloor \mathbf{p}_i^T\dot{\mathbf{x}} \rfloor - k_i\mathbf{p}_i^T\mathbf{x})$$

The workspace is centered at $\mathbf{0}$. The arm is modeled as anisotropic point mass in endpoint space with inertia matrix M, the force exerted against external objects is $\mathbf{f}$, and all $\mathbf{p}_i$s are assembled in the columns of the matrix P. The distribution of force directions $\mathbf{p}_i$ can be arbitrary. Adding the forces generated by all muscles and using Newton's second law yields

$$P(W\mathbf{c}(t-\Delta) - \mathrm{Diag}(\mathbf{b}(\dot{\mathbf{x}}))P^T\dot{\mathbf{x}}(t) - \mathrm{Diag}(\mathbf{k})P^T\mathbf{x}(t)) = \mathbf{f}(t) + M\ddot{\mathbf{x}}(t)$$

where the ith element of vector $\mathbf{b}(\dot{\mathbf{x}})$ is b_i when $\mathbf{p}_i^T\dot{\mathbf{x}} > 0$, and 0 otherwise. Assuming that system-level stiffness and damping are dominated by muscle (rather than passive, joint) properties, the endpoint stiffness and damping matrices are $K = P\,\mathrm{Diag}(\mathbf{k})P^T$ and $B = P\,\mathrm{Diag}(\mathbf{b}(\dot{\mathbf{x}}))P^T$. Expanding the brackets and moving the impedance terms to the right hand side, the constraint on $\mathbf{c}(t-\Delta)$ becomes

$$PW\mathbf{c}(t-\Delta) = \mathbf{f}(t) + M\ddot{\mathbf{x}}(t) + B\dot{\mathbf{x}}(t) + K\mathbf{x}(t) \qquad (4)$$

Because experimental measurements of M, B and K in monkeys are not available, I use approximate values for the human arm, which are probably scaled-up versions[24]. I assume that synaptic weights W onto muscles, and joint torque magnitudes for unit muscle activation do not vary

systematically with endpoint force direction. Thus the only anisotropy in *PW* results from multijoint mechanics; that is, the magnitudes of the column vectors in the matrix *PW* will be larger along the hand–shoulder (*y*) axis because of the Jacobian transformation. Then *PW* can be approximated by $F_{2\times2}U_{2\times\text{Cells}}$, where the columns of *U* are unit length vectors and *F* is a 'force matrix' that stretches column vectors from *U* pointing along the y axis. Other possible sources of anisotropy can also be absorbed in *F*. The ellipsoids corresponding to *M*, *B* and *K* are also elongated along the *y* axis[44,45]; this holds for *M*, as the elbow points downward in typical center-out reaching tasks. As all four ellipsoids have similar orientations and aspect ratios, it will be assumed for simplicity that they are proportional to each other: $M = mF$, $B = bF$, $K = kF$, $|F| = 1$. Then equation 4 can be rewritten as equation 1. A strictly causal model must explain how the motor system 'knows' what the behavior $\mathbf{f}(t)$, $\ddot{\mathbf{x}}(t)$, $\dot{\mathbf{x}}(t)$, $\mathbf{x}(t)$ will be after a delay Δ to generate the MI output $\mathbf{c}(t-\Delta)$. One possibility which is particularly attractive from a control point of view[40] is that $\mathbf{f}(t)$, $\ddot{\mathbf{x}}(t)$ are set to desired external force and acceleration, whereas $\dot{\mathbf{x}}(t)$, $\mathbf{x}(t)$ are set to predicted velocity and position. Such predictions could be obtained from a Kalman-like filter[46]—using delayed sensory feedback, an efference copy of recent motor commands and a forward model of the motor periphery.

Joint space formulation. I have adopted an endpoint formulation, because MI data is traditionally presented in endpoint space and joint angles not even recorded (the differences over a small workspace are likely to be minimal[47]). The formulation of the model in joint space is very similar. Using a local linearization, $B_\theta = J^T B_x J$ and $\dot{\mathbf{x}} = J\dot{\theta}$, so $B_\theta\dot{\theta} = J^T B_x\dot{\mathbf{x}}$ (similarly for the $\ddot{x}$ and $\mathbf{x}$ terms). The joint space equivalent of equation 1 is

$$\mathrm{T}\mathbf{c} = J^T(\mathbf{f} + M_x\ddot{\mathbf{x}} + B_x\dot{\mathbf{x}} + K_x\mathbf{x}) + \mathbf{g}(\theta,\dot{\theta})$$

where the matrix of cell-torque directions T replaces *U*, $\mathbf{g}$ is a Coriolis term, and the Jacobian J^T replaces F^{-1}. Thus F^{-1} is well defined even in the case of mechanical redundancy.

Optimality of cosine tuning. Consider a continuous family of isometric force generators indexed by $\alpha \in [0;2\pi]$ with activation levels $c(\alpha) \in R$ and unit force directions $\mathbf{u}(\alpha) \in R^2$. Each generator contributes force $(c(\alpha) + z(\alpha))\mathbf{u}(\alpha)$, where $z(\alpha)$ are independent random variables (neuromotor noise) with $\mathrm{Var}(z(\alpha)) = c(\alpha)^2$ as observed experimentally[48]. Then the net force is $\mathbf{w} = \int(c(\alpha) + z(\alpha))\mathbf{u}(\alpha)d\alpha$. What activation profile $c(\alpha)$ minimizes $\mathrm{Var}(\mathbf{w}) = \int c(\alpha)^2$ for specified mean force $\mathbf{r} = \int c(\alpha)\mathbf{u}(\alpha)d\alpha$ and specified $C = \int c(\alpha)d\alpha$ coactivation? From Parseval's theorem $\int c(\alpha)^2 = a_0^2 + \sum_{k=1}^{\infty} a_k^2 + b_k^2$, where $a...,b...$ are the Fourier series coefficients of $c(\alpha)$. The constraints given by $\mathbf{r}$, *C* fix the values of a_0, a_1 and b_1, so the infinite sum is minimized when all other terms are 0. Thus a cosine centered on the specified force direction is the optimal activation profile that minimizes expected error but achieves (on average) the specified force and coactivation.

Acknowledgements

I thank Zoubin Ghahramani and Stephen Scott for their suggestions.

Received 21 September 1999; accepted 15 February 2000

1. Evarts, E. V. in *Handbook of Physiology* (ed. Brooks, V. B.) 1083–1120 (Williams and Wilkins, Baltimore, 1981).
2. Johnson, P. B. in *Control of Arm Movement in Space: Neurophysiological and Computational Approaches* (eds. Caminiti, R., Johnson, P. B. & Burnod, Y.) (Springer, Berlin, 1992).
3. Evarts, E. Relation of pyramidal tract activity to force exerted during voluntary movement. *J. Neurophysiol.* **31**, 14–27 (1968).
4. Dum, R. P. & Strick, P. L. The origin of corticospinal projections from the premotor areas in the frontal lobe. *J. Neurosci.* **11**, 667–669 (1991).
5. Fetz, E. E. & Cheney, P. D. Postspike facilitation of forelimb muscle activity by primate corticomotoneuronal cells. *J. Neurophysiol.* **44**, 751–772 (1980).
6. Georgopoulos, A., Kalaska, J., Caminiti, R. & Massey, J. On the relations between the direction of two-dimensional arm movements and cell discharge in primate motor cortex. *J. Neurosci.* **2**, 1527–1537 (1982).
7. Schwartz, A. B. Direct cortical representation of drawing. *Science* **265**, 540–542 (1994).
8. Moran, D. W. & Schwartz, A. B. Motor cortical representation of speed and direction during reaching. *J. Neurophysiol.* **82**, 2676–2692 (1999).
9. Kalaska, J. F., Cohen, D. A. D., Hyde, M. L. & Prud'homme, M. A comparison of movement direction-related versus load direction-related activity in primate motor cortex, using a two-dimensional reaching task. *J. Neurosci.* **9**, 2080–2102 (1989).
10. Sergio, L. E. & Kalaska, J. F. Changes in the temporal pattern of primary motor cortex activity in a directional isometric force versus limb movement task. *J. Neurophysiol.* **80**, 1577–1583 (1998).
11. Kettner, R. E., Schwartz, A. B. & Georgopoulos, A. P. Primate motor cortex and free arm movements to visual targets in three-dimensional space III. Positional gradients and population coding of movement direction from various movement origins. *J. Neurosci.* **8**, 2938–2947 (1988).
12. Flament, D. & Hore, J. Relations of motor cortex neural discharge to kinematics of passive and active elbow movements in the monkey. *J. Neurophysiol.* **60**, 1268–1284 (1988).
13. Thach, W. T. Correlation of neural discharge with pattern and force of muscular activity, joint position, and direction of intended next movement in motor cortex and cerebellum. *J. Neurophysiol.* **41**, 654–676 (1978).
14. Alexander, G. E. & Crutcher, M. D. Neural representations of the target (goal) of visually guided arm movements in three motor areas of the monkey. *J. Neurophysiol.* **64**, 164–178 (1990).
15. Fu, Q.-G., Flament, D., Coltz, J. D. & Ebner, T. J. Temporal encoding of movement kinematics in the discharge of primate primary motor and premotor neurons. *J. Neurophysiol.* **73**, 836–854 (1995).
16. Hocherman, S. & Wise, S. P. Effects of hand movement path on motor cortical activity in awake, behaving rhesus monkeys. *Exp. Brain Res.* **83**, 285–302 (1991).
17. Humphrey, D. R. & Reed, D. J. in *Advances in Neurology: Motor Control Mechanisms in Health and Disease* (ed. Desmedt, J. E.) 347–372 (Raven, New York, 1983).
18. Carpenter, A. F., Georgopoulos, A. P. & Pellizzer, G. Motor cortical encoding of serial order in a context-recall task. *Science* **283**, 1752–1757 (1999).
19. Georgopoulos, A. P., Lurito, J. T., Petrides, M., Schwartz, A. B. & Massey, J. T. Mental rotation of the neuronal population vector. *Science* **243**, 234–236 (1989).
20. Scott, S. & Kalaska, J. Changes in motor cortex activity during reaching movements with similar hand paths but different arm postures. *J. Neurophysiol.* **73**, 2563–2567 (1995).
21. Ashe, J. & Georgopoulos, A. P. Movement parameters and neural activity in motor cortex and Area 5. *Cereb. Cortex* **6**, 590–600 (1994).
22. Fetz, E. E. Are movement parameters recognizably coded in the activity of single neurons? *Behav. Brain Sci.* **15**, 679–690 (1992).
23. Joyce, G. C., Rack, P. M. H. & Westbury, D. R. The mechanical properties of cat soleus muscle during controlled lengthening and shortening movements. *J. Physiol. (Lond.)* **204**, 461–474 (1969).
24. Zajac, F. E. Muscle and tendon: properties, models, scaling, and application to biomechanics and motor control. *Crit. Rev. Biomed. Eng.* **17**, 359–411 (1989).
25. Winter, D. A. Biomechanics and Motor Control of Human Movement (Wiley, New York, 1990).
26. Hubel, D. H. & Wiesel, T. N. Receptive fields, binocular interaction and functional architecture in the cat's visual cortex. *J. Physiol. (Lond.)* **160**, 106–154 (1962).
27. Crammond, D. J. & Kalaska, J. F. Differential relation of discharge in primary motor cortex and premotor cortex to movements versus actively maintained postures during a reaching task. *Exp. Brain Res.* **108**, 45–61 (1996).
28. Kalaska, J. F. & Crammond, D. J. Cerebral cortical mechanisms of reaching movements. *Science* **255**, 1517–1523 (1992).
29. Kalaska, J. F., Crammond, D. J., Cohen, D. A. D., Prud'homme, M. & Hyde, M. L. in *Control of Arm Movement in Space: Neurophysiological and Computational Approaches* (eds. Caminiti, R., Johnson, P. B. & Burnod, Y.) (Springer, Berlin, 1992).
30. Taira, M., Boline, J., Smyrnis, N., Georgopoulos, A. & Ashe, J. On the relations between single cell activity in the motor cortex and the direction and magnitude of three-dimensional static isometric force. *Exp. Brain Res.* **109**, 367–376 (1996).
31. Bennett, D. J., Hollerbach, J. M., Xu, Y. & Hunter, I. W. Time-varying stiffness of human elbow joint during cyclic voluntary movement. *Exp. Brain Res.* **88**, 433–442 (1992).
32. Bullock, D., Cisek, P. & Grossberg, S. Cortical networks for control of voluntary arm movements under variable force conditions. *Cereb. Cortex* **8**, 48–62 (1998).
33. Caminiti, R., Johnson, P. & Urbano, A. Making arm movements within different parts of space: dynamic aspects in the primate motor cortex. *J. Neurosci.* **10**, 2039–2058 (1990).
34. Scott, S. & Kalaska, J. Reaching movements with similar hand paths but different arm orientation. I. Activity of individual cells in motor cortex. *J. Neurophysiol.* **77**, 826–852 (1997).
35. Tanaka, S. Hypothetical joint-related coordinate systems in which populations of motor cortical neurons code direction of voluntary arm movements. *Neurosci. Lett.* **180**, 83–86 (1994).

36. Kakei, S., Hoffman, D. & Strick, P. Muscle and movement representations in the primary motor cortex. *Science* **285**, 2136–2139 (1999).
37. Fetz, E. E., Cheney, P. D., Mewes, K. & Palmer, S. Control of forelimb muscle activity by populations of corticomotoneuronal and rubromotoneuronal cells. *Prog. Brain Res.* **80**, 437–449 (1989).
38. Miller, L. E. & Sinkjaer, T. Primate red nucleus discharge encodes the dynamics of limb muscle activity. *J. Neurophysiol.* **80**, 59–70 (1998).
39. Gottlieb, G. L. On the voluntary movement of compliant (inertial-viscoelastic) loads by parcellated control mechanisms. *J. Neurophysiol.* **76**, 3207–3228 (1996).
40. Khatib, O. A unified approach to motion and force control of robotic manipulators: the operational space formulation. *IEEE J. Robotics Automat.* **RA-3**, 43–53 (1987).
41. Scott, S. H. Comparison of onset time and magnitude of activity for proximal arm muscles and motor cortical cells before reaching movements. *J. Neurophysiol.* **77**, 1016–1022 (1997).
42. Bizzi, E., Mussa-Ivaldi, F. A. & Giszter, S. F. Computations underlying the execution of movement: a biological perspective. *Science* **253**, 287–291 (1991).
43. Galagan, J. Spinal Mechanisms of Motor Control. Thesis, MIT (1999).
44. Tsuji, T., Morasso, P. G., Goto, K. & Ito, K. Human hand impedance characteristics during maintained posture. *Biol. Cybern.* **72**, 475–485 (1995).
45. Gomi, H. & Kawato, M. Equilibrium-point control hypothesis examined by measured arm stiffness during multijoint movement. *Nature* **272**, 117–120 (1996).
46. Wolpert, D., Gharahmani, Z. & Jordan, M. An internal model for sensorimotor integration. *Science* **269**, 1880–1882 (1995).
47. Mussa-Ivaldi, F. A. Do neurons in the motor cortex encode movement direction? An alternative hypothesis. *Neurosci. Lett.* **91**, 106–111 (1988).
48. Schmidt, R. A., Zelaznik, H., Hawkins, B., Frank, J. S. & Quinn, J. T. J. Motor-output variability: a theory for the accuracy of rapid motor acts. *Psychol. Rev.* **86**, 415–451 (1979).
49. Sanes, J. N. & Shadmehr, R. Sense of muscular effort and somatesthetic afferent information in humans. *Can. J. Physiol. Pharmacol.* **73**, 223–233 (1995).
50. Fu, Q.-G., Suarez, J. & Ebner, T. Neuronal specification of direction and distance during reaching movements in the superior precentral premotor area and primary motor cortex of monkeys. *J. Neurophysiol.* **70**, 2097–2116 (1993).

Population vectors and motor cortex: neural coding or epiphenomenon?

Stephen H. Scott

A simple model suggests that activity in primary motor cortex may encode the activity of individual muscles and not higher-order features as previously suspected.

The primary motor cortex (M1) plays a pivotal role in controlling volitional movement, yet there is considerable debate as to how best to interpret neural activity in this brain region. The traditional approach, first introduced by Ed Evarts almost forty years ago, relates the activity of motor cortical neurons to variables such as movement or force at individual joints. A second approach, introduced by Apostolos Georgopoulos and colleagues in the early 1980s, is based mainly on studies in which monkeys make an arm movement to reach for a target; this approach relates M1 activity to the movement of the hand rather than of the individual joints (such as the shoulder and elbow) that contribute to the movement. Neurons in M1 are broadly tuned to the direction of hand movement[1], with each neuron having a preferred direction of movement for which its firing rate is maximal; Georgopoulos and colleagues showed[2] that a population vector constructed from the firing rates of many cortical neurons tends to point in the direction of the hand movement (see **Fig. 1** for theory). Subsequent work from various laboratories has used this hand-based framework to demonstrate impressive relationships between hand motion and neural activity, at both the single-cell and population levels.

These correlations have been interpreted as suggesting that the motor cortex controls higher-level features of hand movements, rather than the lower-level features related to the individual joints and muscles that bring about those movements. This interpretation has important implications not only for understanding M1 but also for the role of other parts of the motor system that lie hierarchically above (dorsal premotor cortex) or below (spinal cord) the motor cortex. For example, if M1 represents hand movements using a population code, then the conversion of this relatively abstract representation into commands to the specific muscles would have to occur downstream, presumably in the spinal cord.

The article by Todorov[3] on page 391 of this issue challenges this view. The author's thesis—which seems certain to be controversial—is that many of the previously-described correlations between motor cortical activity and hand motion can be explained with a simple model in which the activity of cortical neurons encodes the activation of a group of muscles. This is not a radically new hypothesis to the field, nor is it a complete account of the motor cortex. The strength of Todorov's model, however, lies in its demonstration that so many observations from the previous literature can be accounted for by the complexity of the musculoskeletal system.

The relationship between arm muscle activity and hand motion is not trivial. Classical studies of muscle physiology have shown that the relationship between a muscle's activity (that is, the firing rate of its motor units) and its force output is strongly dependent on muscle velocity and length. Furthermore, the conversion of muscle force to hand motion depends on the geometry of the limb, its inertial properties and the presence of external loads. Todorov's model incorporates these various factors (albeit in a simplified form) in order to calculate the patterns of cortical activity that would be associated with various whole-limb motor tasks, assuming that cortical neurons encode muscle activation. One result of the model is that population vectors tend to point in the direction of movement, simply because of the balance that exists between the various mechanical factors related to muscle and limb dynamics. The model also predicts that the direction of the population vector will no longer point in the direction of movement if one disturbs this natural balance. This prediction is supported by experiments[4] in which monkeys performed reaching movements while pulling against a mechanical load whose direction could vary. In this situation, the mechanical action of the load at the hand requires greater muscular torque (or muscle activity) at the joints when loads are applied in a lateral as compared to a sagittal direction. Todorov's model[3] predicts that population vectors will be skewed laterally under these conditions, and this is what was observed[4].

A more complex and surprising property of Todorov's model is its ability to account for differences in the relative timing of motor output and motor cortical

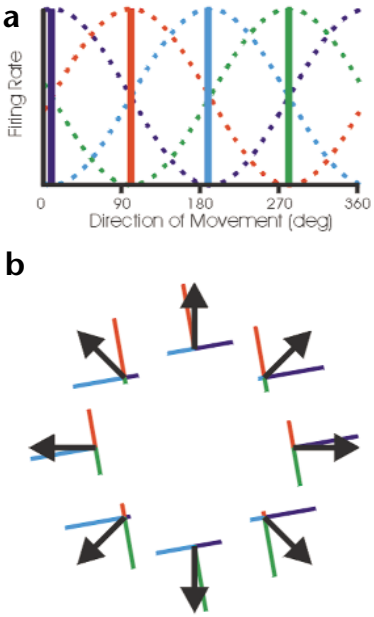

Fig. 1. The construction of a population vector from the firing rates of cells. (**a**) The activities of motor cortical neurons tend to be broadly tuned to the direction of movement (dashed lines). The solid vertical lines denote the preferred direction (PD) of each cell, the movement direction for which that cell is maximally active. (**b**) For each movement direction, the activity of each cell scales the length of a vector aligned with its PD, and the vector sum of all cells defines a population vector. It has been shown that this population vector will predict the direction of movement if three conditions are met. First, neural activity is broadly tuned to the direction of movement; second, the PDs of the cells are uniformly distributed in space; and third, there is no systematic relationship between a cell's discharge rate and its preferred direction[8,9].

Stephen Scott is in the Department of Anatomy and Cell Biology, Queen's University, Kingston, Ontario, Canada K7L 3N6
e-mail: steve@biomed.queensu.ca

activity as defined by the population vector. When monkeys make circular arm movements (whose direction changes continuously), the direction of the hand was found to lag behind that of the population vector, with a time interval that varied with the degree of curvature[5]. For tight circles, the lag was about 100 ms, but for large circles the lag was only 30 ms. These results were interpreted as evidence that the motor cortex is involved in controlling movements with high curvature, but not movements that are more straight. Todorov's model, however, predicts the exact same time differences between the population vector and hand movement, even while assuming a fixed time lag between the firing of the cortical neurons and the activation of the muscles. This is because the interplay between the mechanical properties of the musculoskeletal system related to length, velocity and acceleration create a systematic temporal shift between population vector direction and hand motion. In other words, the mechanical complexity of the limb leads to complexity of the population vector.

Todorov's article also illustrates some of the pitfalls that can occur when statistical approaches are used to correlate neural activity with different movement parameters. Various investigators have used multiple regression techniques to look for parameters of hand movement that show correlations with neural activity. A common finding has been that many parameters show some correlation, but that the correlations are greatest for movement direction and smallest for acceleration[6]. Because acceleration is tightly linked to force (according to Newtonian mechanics), this finding has been interpreted as suggesting that force is not among the major parameters coded by M1. Todorov shows, however, that a muscle-based model predicts virtually the same results: high correlations with movement direction and low correlations with acceleration. The model also predicts that, because of the force-velocity relationship of muscle, neural activity should also correlate with hand velocity; this too has been observed experimentally[7]. Finally, Todorov illustrates how the methods used to analyze neural data can have considerable consequences for the observed correlations. Specifically, squaring the discharge rate of neurons in order to stabilize the variance (as is commonly done; see for instance ref. 6), causes a dramatic increase in the percentage of neurons that appear to represent movement direction (from 17% to 43% in Todorov's model). This implies that previous studies may have overestimated the representation of movement direction in M1; indeed, Todorov suggests that many of the previously described correlations may be epiphenomenal, given that similar correlations arise in his model even though movement direction is never specified directly.

The new model is not meant to capture all the nuances of motor cortical activity during movement, and it does not prove that motor cortical activity is devoid of all higher-level features of movement related to the hand. It does, however, demonstrate two important points. First, even the simplest model of motor cortical function, treating it as a generator of muscle activity patterns, can lead to unanticipated and complex correlates of hand motion due to the mechanical properties of the limb and its musculature. Second, given these complexities, the relationship between neural activity and limb movement is not easily determined. Therefore, before concluding that brain activity reflects complex representations of movement, the data must be scrutinized to ensure that the observed correlations are not merely a reflection of properties of the peripheral motor apparatus. Engineers have to understand the plant before they can figure out how to control it. Why should it be any different when examining biological control?

1. Georgopoulos, A. P., Kalaska, J. F., Caminiti, R. & Massey, J. T. *J. Neurosci.* **2**, 1527–1537 (1982).
2. Georgopoulos, A. P. Caminiti, R. Kalaska, J. F. & Massey, J. T. *Exp. Brain Res. Suppl.* **7**, 327–336 (1983).
3. Todorov, E. *Nat. Neurosci.* **3**, 391–398 (2000).
4. Kalaska, J. F., Cohen, D. A. D., Hyde, M. L. & Prud'Homme, M. *J. Neurosci.* **9**, 2080–2102 (1989).
5. Moran, D. W. & Schwartz, A. B. *J. Neurophysiol.* **82**, 2693–2704 (1999).
6. Ashe, J. & Georgopoulos, A. P. *Cereb. Cortex* **6**, 590–600 (1994).
7. Moran, D. W. & Schwartz, A. B. *J. Neurophysiol.* **82**, 2676–2692 (1999).
8. Mussa-Ivaldi, F. A. *Neurosci. Lett.* **91**, 106–111 (1988).
9. Sanger, T. *Neural Computation* **6**, 29–37 (1994).

A signal for synapse formation

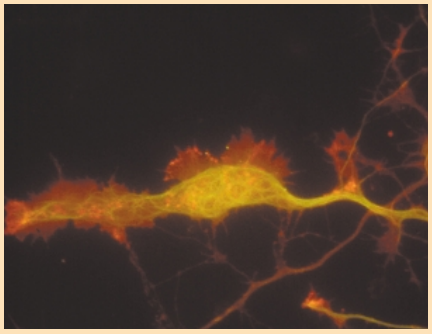

When growth cones reach their synaptic targets, they must both send and receive signals in order to promote formation of mature synapses. We know little about the identity of such signals, but a recent paper (Hall, A.C., Lucas, F.R. & Salinas, P.C. *Cell* **100**, 525–535, 2000) offers provocative evidence that WNT-7a may be one such molecule. The WNT factors are a family of secreted signaling proteins, and are known to be involved in early developmental patterning. Several are also expressed in the brain, and the presence of WNT-7a in cerebellar granule cells during the period of synaptogenesis prompted the authors to examine a possible role in this process.

Hall *et al.* studied the formation of synapses between mossy fibers, originating in the pons, and granule cells. Cultured granule cells secrete factors that induce remodeling of pontine axons *in vitro*; the effects include a spreading of the growth cones, changes in their cytoskeletal structure and an increase in filopodial length. These effects were blocked by an antagonist of WNT signaling, and were mimicked by conditioned medium containing WNT-7a (the figure shows a treated growth cone, stained for GAP-43, red, and tubulin, green). Remodeling could also be induced by low concentrations of lithium, which mimics WNT signaling by inhibiting a downstream kinase called GSK-3β. Finally, mice lacking WNT-7a show a delay in the formation of mossy fiber-granule cell synapses *in vivo*. The synapses do form eventually, suggesting that other members of the WNT family might be able to substitute for WNT-7a, but the phenotype nevertheless indicates that WNT-7a is involved in this process. It will be interesting to determine whether WNT factors play similar roles at other synapses, and whether they are also involved in adult plasticity. It will also be interesting to know whether any of the clinical effects of lithium (used to treat manic depression) can be attributed to its effects on WNT signaling.

Charles Jennings

One motor cortex, two different views

TO THE EDITOR—In a recent paper in *Nature Neuroscience*, Todorov[1] referred to our finding that a motor cortical representation of hand trajectory during spiral drawing precedes the hand's movement by an interval that varies with path curvature[2,3]. Although there are several possible explanations for this finding, Todorov, using a simplistic model, argued that because cortical cells share common properties with muscles, this relationship could be due to a combination of inertia, viscosity and stiffness acting on the acceleration, speed and position of the arm, respectively. Although simple, his model is flawed and cannot support this conclusion.

The author models a multijoint arm as a simple cantilever that is converted to single point-mass equation using a Jacobian transformation (web supplement A, http://www.nature.com/neuro/web_specials/). The arm's properties were derived from a simplified version of muscle whose activity is a linear combination of motor cortical activity. This model was used to reinterpret our results[2,3]. In our study, monkeys drew spirals on a vertically oriented computer touchscreen. The center of the spiral was located in front of the monkey, between its shoulders. According to Todorov's model, this location corresponded to the equilibrium point of the arm—the location where the parameters in his model would force the arm to rest. Todorov assumed that cortical activity reflects the inertia, viscosity and stiffness of the arm and showed that his model produces the same variable lags as our cortical population vectors. However, any acceleration representation in the cortical activity would actually decrease lags as a function of curvature, which is exactly opposite to our finding (web supplement B, http://www.nature.com/neuro-/web_specials/).

The increased lag with increasing curvature shown in Todorov's article is due to his positional term. The idea that extrinsic position may be a factor in motor cortical activity is not new[4–6]. However, Todorov's method of equating extrinsic position representation to muscle stiffness is incorrect. This model assumes that muscle viscoelastic properties are independent of muscle activation. Thus, even an inactivated muscle will act as a large spring pulling the arm back to some equilibrium position. In real muscle, the force–length and force–velocity relationships are modulated by muscle activation such that at zero activation, the muscle is essentially a non-force producer. In the real world, the combination of gravity and inactive muscles will force the arm to fall to the side. In Todorov's model, the combined effect of gravity and muscle stiffness on inactive muscles would make the hand float at mid-chest level; muscle activity would be required to force the arm down below chest level. This, of course, is unrealistic. Viscoelastic models like the ones used by Todorov are only valid for perturbation studies where both posture and neural activity are assumed to be constant. Using such equations to solve for time-varying muscle activations violates the basic assumptions of perturbation models. Simple dynamic models can be useful to explain arm mechanics. However, when the models are not consistent with basic physiology, exclude important phenomena, and violate inherent assumptions, they cannot be compared to empirical data.

Daniel W. Moran and Andrew B. Schwartz
The Neurosciences Institute, 10640 John Jay Hopkins Drive, San Diego, California 92121, USA
email: dmoran@nsi.edu or aschwartz@nsi.edu

TO THE EDITOR—Here we refute claims by Todorov[1] and Scott[7] that the importance of target direction as an explanatory factor for cortical activity in a regression analysis we performed[5] is an 'artifact' of a square-root transformation of neural discharge rates. Specifically, it was touted by Scott[7] that "squaring [*sic*] the discharge rate of neurons in order to stabilize the variance ... causes a dramatic increase in the percentage of neurons that appear to represent movement direction (from 17% [*sic*] to 43% in Todorov's model)." The data to which Todorov[1] referred concerned the percentages of cells for which a particular variable yielded the highest R^2 when used alone in the regression. We re-analyzed these data using the regression analysis we used previously[5] but without any transformation of the discharge rate. The results of the two analyses were practically identical, the average absolute difference being only 1.9% (http://www.nature.com/neuro/web_specials/). However, there was a statistically significant improvement of the regression fit when the square-root transformation was used. The median R^2 for the square-root transformed data was 0.5811, as compared to 0.544 for the non-transformed data ($P < 0.0001$, Wilcoxon's signed-rank test). This was anticipated, because the square-root transformation is expected to make the distribution of counts more symmetrical. This transformation is routinely used when analyzing counts[8–10], given the commonly highly skewed distribution of such data. Finally, we analyzed the data without any transformation or smoothing. In this case, the agreement with the original analysis was even closer, the average absolute difference being only 0.86%. We conclude that the relationship between neural activity and movement parameters found earlier[5] holds irrespective of the specific transformation and/or smoothing used. Finally, while we dealt above with the issue of square-root transformation because of the more general importance of this transformation for analyzing neuronal spike counts, there are also numerous other points raised by Todorov[1] which we also dispute, including the force direction/magnitude issue, which we cannot critically discuss due to space limitations.

Apostolos P. Georgopoulos and James Ashe
Brain Sciences Center, Veterans Affairs Medical Center and Department of Neuroscience, University of Minnesota Medical School, Minneapolis, Minnesota 55417, USA
email (A.P.G): omega@tc.umn.edu

REPLY TO MORAN AND SCHWARTZ—Assuming that M1 cells control the activation of muscle groups, I have previously derived an equation[1] relating the M1 population vector (PV) to hand kinematics and kinetics. In addition to force and acceleration terms, this equation includes velocity and positional terms needed to compensate for muscle visco-elasticity. The interplay among these terms offers a simple explanation to several puzzling phenomena[1] including the curvature-dependent time-lag between PV direction and tangential velocity[2,3]. The strength of the model is that multiple phenomena are explained simultaneously, using the most basic properties of the musculoskeletal apparatus and thus avoiding the danger of curve fitting.

Moran and Schwartz claim that the fit to their data[2,3] is somehow an artifact of the approximation I used, and that the results will change if additional details are considered. It is not explained how a first-oreer approximation could produce such

artifacts. The absence of gravity and activation-dependent stiffness in my model are discussed at length, without any explanation as to why adding them should change the results. Unlike hand acceleration, which is time-varying, the gravitational force is roughly constant for small variations in limb configuration. Therefore, its effect is absorbed in the baseline (defined as postural activity in the center of the workspace). The constant stiffness approximation is reasonable once a certain activation level is reached[11]. It is true that setting stiffness to zero abolishes the time lag–curvature effect; however, that point is irrelevant—whether or not muscle stiffness is constant, it certainly exists and there is no justification for setting it to zero. To compensate for muscle stiffness, M1 cells have to exhibit well-documented positional gradients—which, in combination with the acceleration term, produce the negative time lag–curvature relationship[1].

Moran and Schwartz have only shown that my model is approximate—which is very different from being "flawed." Still, is it possible that the results are an artifact of the approximation, for reasons that these authors did not identify? To assess the sensitivity to previously unmodeled details, I repeated the analysis using a state-of-the-art muscle model[12] (http://www.nature.com/neuro/web_specials/). Muscle force was expressed as a complex function of muscle length, velocity and stimulation frequency; this function depends on 19 experimentally derived parameters and incorporates numerous results from muscle physiology[12]. For a wide range of parameters, the predicted relationship between PV time lag and path curvature was quantitatively similar to the original result[1] as well as to the experimental data[2,3]. Thus, when Moran and Schwartz wrote that my model "is not consistent with basic physiology, excludes important phenomena, and violates inherent assumptions," their concerns were misplaced.

REPLY TO GEORGOPOULOS AND ASHE—In their letter, Georgopoulos and Ashe address the issue of whether data preprocessing affects M1 cell classification. Their results do not refute my main point[1], which is that previous classification procedures[5,13] can be seriously biased—with or without data preprocessing. Here I focus on the procedure[5] for classifying cells as direction- (D), position- (P), velocity- (V) or acceleration-related (A) according to the largest R^2.

By definition, the bias of a statistical estimator is the expected difference between the correct and estimated values of a given parameter. The identical percentages found by Georgopoulos and Ashe with and without data preprocessing only prove that, for this particular dataset, the bias is equal in both cases. The value of this bias cannot be inferred from their results (or anything else computed on real data), because the correct answer is unknown. In the absence of analytical insight, the only way to identify the bias of an estimator is to apply it to synthetic datasets where the correct answer is known. When applied to synthetic data[1] with no separate directional component, the above classification procedure finds D 43%, V 39%, P 16%, A 2% on smoothed square-root-transformed spike trains, and D 26%, V 56%, P 16%, A 2% on raw binned spike trains (different from continuous mean firing rates which were labelled MFR previously[1]). The effects of the data transformation (8% on average) are to be expected in general, and could exist in other datasets. With or without the transformation, the above percentages are very far from the correct answer: D 0%, V 49%, P 46%, A 5%—that is, the classification procedure itself is biased. Thus the burden of proof lies on Georgopoulos and Ashe. Unless they identify the exact conditions under which their procedure is unbiased, and ascertain by independent means that these conditions hold for the M1 population, their results remain hard to interpret.

To gain more insight into why the R^2 classification procedure fails, I analyzed the family of synthetic responses misclassified as directional (http://www.nature.com/neuro/web_specials/). These responses do not look directional: the temporal fluctuations of the underlying position, velocity and acceleration terms do not cancel out. The artificially created 'directional' region of parameter space is centered at the point where the correct classification boundaries meet. Therfore responses are misclassified as directional just because they do not fit well in the other categories. It would be interesting to re-analyze the data of Georgopoulos and Ashe for that possibility. Do responses labeled as directional vary only with movement direction and contain no systematic temporal fluctuations (which is how a truly directional cell should behave), or do they fluctuate over time in ways that do not happen to fit in any of the alternative categories? The latter type of response is more properly labeled 'unknown' rather than 'directional.'

Finally, this debate obscures a more fundamental problem[1,14] with M1 cell classification, a problem that remains even if unbiased procedures are developed. The different components of the cell response are not fixed, but instead increase monotonically with the magnitude of the corresponding kinematic and kinetic terms. Thus a cell classified in one task as 'velocity-related' could become 'position-related' in another task if the movement is slow enough, 'acceleration-related' if the movement is fast enough, and 'load-related' if a large enough external load is imposed (http://www.nature.com/neuro/web_specials/). Given this sensitivity to task parameters, classifying M1 cells according to the largest component of their response should perhaps be avoided altogether.

Emanuel Todorov
Gatsby Computational Neuroscience Unit, University College London, 17 Queen Square London WC1N 3 AR, UK
email: emo@gatsby.ucl.ac.uk

REPLY—The article by Todorov[1] and associated letters illustrate clear opinion differences regarding the function of motor cortex during goal-directed arm movements. This controversy is partially generated by the different experimental protocols used to examine motor cortex function in non-human primates. The first, introduced by Evarts, examines single-joint movements and relates neural activity to muscle-based or joint-based variables[15]. The second, introduced by Georgopoulos, examines whole-arm movements and relates neural activity to hand-based variables[16]. Practitioners of the former find correlates of muscle-based or joint-based variables; practitioners of the latter find correlates of hand-based variables.

T. S. Kuhn captures the present situation: "proponents of competing paradigms practice their trades in different worlds ... the two groups of scientists see different things when they look from the same point in the same direction."[17] With regard to motor cortex function, neural correlates of hand direction are seen as evidence by one group that hand direction is an important and potentially dominant signal, whereas the other group views this observation as an obvious by-product of neural activity that controls muscles to move the limb.

These differences of opinion are important for understanding not only the function of motor cortex, but also the function of other cortical and subcortical regions of the CNS, such as the spinal cord. At the extremes, the spinal cord could be viewed as the central location where all decisions on the details of motor selection are generated from a simple descending command specifying the global goal of the task. Alter-

natively, it could be viewed as evolutionary baggage that simply conducts fully orchestrated signals generated in higher motor regions onto motoneurons. As usual, the truth likely lies in the middle.

Todorov states that many neural correlates of hand-based variables can be explained if motor cortical activity simply encoded muscle activation patterns. Related arguments have been proposed for neural correlates of mental rotation in motor cortex[18]. Neither of these articles disprove that neural activity reflects hand-related or cognitive functions; they simply demonstrate that there are alternative interpretations for these experimental observations. Although one can argue whether Todorov's model can predict the details of each hand-based correlate, this muscle-based model reveals how little we know about the function of motor cortex during whole-limb motor tasks.

Although the model by Todorov challenges the use of hand-based frameworks for interpreting motor cortical activity, it is important to recognize the technical difficulty of these experiments. It was a logical and sensible decision to relate neural activity to movements of the hand when Georgopoulos and colleagues introduced this paradigm over 20 years ago[16]. This hand-based model has provided an influential contribution to both motor and cognitive neuroscience. However, substantial progress in our understanding of the function of primary motor cortex now requires a change in the experimental framework[19]. Such a change must allow for exploration of the rich and diverse activation patterns of motor cortical neurons related not only to global features of the task, but also to features of movement related to the peripheral motor apparatus.

Stephen H. Scott
Dept. of Anatomy and Cell Biology, Queen's University, Kingston, Ontario K7L 3N6, Canada
e-mail: steve@biomed.queensu.ca

1. Todorov, E. *Nat. Neurosci.* 4, 391–398 (2000).
2. Schwartz, A. B. *Science* 265, 540–542 (1994).
3. Moran, D.W. & Schwartz, A. B. *J. Neurophysiol.* 82, 2693–2704 (1999).
4. Kettner, R. E., Schwartz, A. B. & Georgopoulos, A. P. *J. Neurosci.* 8, 2938–2947 (1988).
5. Ashe, J. & Georgopoulos, A. P. *Cereb. Cortex* 6, 590–600 (1994).
6. Fu, Q.-G., Flament, D., Coltz, J. D. & Ebner, T. J. *J. Neurophysiol.* 73, 836–854 (1995).
7. Scott, S. *Nat. Neurosci.* 4, 307–308 (2000).
8. Snedecor, G. W. & Cochran, W. G. *Statistical Methods* (Iowa State Univ. Press, Ames, Iowa, 1989).
9. Cox, D. R. & Lewis, P. A. W. *The Statistical Analysis of Series of Events* (Chapman and Hall, London, 1966).
10. Tukey, J. W. *Exploratory Data Analysis* (Addison-Wesley, Reading, Massachusetts, 1977).
11. Rack, P. & Westbury, D. *J. Physiol. (Lond.)* 204, 443–460 (1969).
12. Brown, I., Cheng, E. & Loeb, G. *J. Muscle Res. Cell Motility* 20, 627–643 (1999).
13. Taira, M., Boline, J., Smyrnis, N., Georgopoulos, A. & Ashe, J. *Exp. Brain. Res.* 109, 367–376 (1996).
14. Fetz, E. *Behav. Brain Sci.* 15, 679–690 (1992).
15. Evarts, E.V. *J. Neurophysiol.* 31,14–27 (1968).
16. Georgopoulos, A. P., Kalaska, J. F., Caminiti, R. & Massey, J. T. *J. Neurosci.* 2 1527–1537 (1982).
17. Kuhn, T. S. *The Structure of Scientific Revolutions* 2nd edn. 150 (University of Chicago Press, Chicago, 1970).
18. Cisek, P. & Scott, S. H. *Neurosci. Lett.* 272, 1–4 (1999).
19. Scott, S. H. *Can. J. Physiol. Pharm.* (in press).

'What', 'where' and 'how' in auditory cortex

TO THE EDITOR—In their commentary on Romanski *et al.*'s findings of (at least) two streams of auditory projections to the prefrontal cortex[1], Kaas and Hackett have suggested that this anatomical segregation reflects, as in visual cortex, a functional segregation of the object-related and space-related aspects of auditory processing ('What' and 'Where,' respectively)[2,3]. This model derives from the increasingly accepted notion that the cortical systems for different sensory modalities may share principles of functional organization[3,4]. However, the 'What/Where' model of auditory functional specialization remains conjectural. In particular, there is little evidence that circumscribed areas of the auditory cortex are specialized to process spatial information[5] or that topographic spatial maps exist in auditory cortex, although such maps do exist in the colliculi[6]. Results suggest that auditory spatial location is represented in the auditory cortex as a distributed code based on spike timing[7].

Here we propose an alternative model of functional segregation in the auditory cortex. Our model agrees that the ventral pathway is probably involved in perceiving auditory objects by extracting 'acoustic signatures,' the invariant set of auditory features that allow identification of sound sources ('What'). However, our model suggests that the dorsal pathway is primarily involved in perceiving the evolution in time of the signal emitted by one or several auditory objects, a process based on accurate analysis of spectral motion (SM, 'Where-in-frequency' or 'How'). SM corresponds to changes in position of the peaks of acoustic energy in frequency space, and is especially present in animal vocalizations (reflecting motion of the vocal apparatus), in particular in speech, where the time-course of the formant frequencies contain most of the phonemic information. Perception of SM is thus an important aspect of auditory cognition, in particular of speech perception, which supports the existence of a dedicated neuronal pathway. Neuroimaging and lesion studies in humans suggest that speech perception is highly dependent on the posterior part of the auditory cortex[8,9] ; this corresponds with the location of the putative 'How' pathway in caudal parts of auditory cortex.

Auditory SM is analogous to visual spatial motion[3]. Both are related to distribution changes of energy across the sensory epithelium: as visual motion corresponds to movements of light on the retina, SM corresponds to movements of acoustic energy across the basilar membrane, along the frequency dimension. Because topographical relationships along the sensory epithelium are conserved up to and beyond primary sensory cortices, our model implies that functions of the dorsal pathways in the auditory and visual cortex are based on similar neuronal computations. Pursuing this analogy, a major processing stage of the caudal auditory pathway could consist of a cortical area sensitive to SM, analogous to visual area V5/MT. Neuroimaging suggests that such an area can be found bilaterally in the posterior part of the superior temporal gyrus, in the presumed caudal pathway[10].

Thus, our model suggests that anatomical segregation in dorsal and ventral auditory pathways reflects two different modes of auditory processing, analogous to those of the visual pathways. Applied to speech perception, our model suggests that the dorsal pathway extracts the verbal message contained in a spoken sentence, while the

Web Supplement A

The author models a multijoint arm as a simple cantilever which is converted to single point-mass equation using a Jacobian transformation. Thus:

$$\sum F_m + F_e = m\ddot{x} \qquad 1$$

where $\boldsymbol{F_m}$ represents individual muscle forces and $\boldsymbol{F_e}$ represents any external forces applied to hand (*e.g.*, manipulandum), $\boldsymbol{m}$ represents the inertia of the arm and $\ddot{x}$ represents hand acceleration. The arm's combined muscle properties were derived from a simplified version of muscle activity defined as:

$$f(a,l,\dot{l}) = a - k(l_0 - l) - \lfloor b\dot{l} \rfloor \qquad 2$$

where $\boldsymbol{f, a, l, l_0}$ represent a single muscle's force, activation, length, and rest length, respectively. Summing Equation 2 over all muscles, and substituting into Equation 1 yields:

$$\sum au + F_e = m\ddot{x} + b\dot{x} + kx \qquad 3$$

where the viscous ($\boldsymbol{b}$) and elastic ($\boldsymbol{k}$) terms are due combined muscle properties. The left term in Equation 3 represents muscle activation (multiplied by the muscle's preferred direction) which the author equates with M1 activity (*i.e.*, a motor cortical cell is an upper motor neuron). Therefore, the first term of Equation 3 represents a motor cortical population vector which, when there are no external forces, is a linear combination of acceleration, velocity and position of the hand.

Web Supplement B

The effect of acceleration on lag in Todorov's formulation can be demonstrated by eliminating the position term (*i.e.*, setting the stiffness coefficient to zero) in his lag equation (Figure 4 caption). Figure 1 shows that increasing acceleration actually decreases lag in drawing tasks. Thus, acceleration has exactly the opposite effect of that needed to explain our observations. Therefore, the increased lags with increasing curvature shown in Figure 4 of Todorov's article are due solely to his positional term. This contrary effect of acceleration is due to the inverse speed-curvature relation characteristic of drawing movements (*i.e.*, $^2/_3$ power law). When drawing the outside of a spiral, acceleration is low and velocity is high; thus, the phase of a weighted signal of velocity and acceleration would lie closer to the velocity signal than the acceleration signal. When the hand is on the inside of the spiral, the opposite is true and a mixed signal would be closer to the acceleration signal in phase. However, because the angular velocity of the movement increases with higher curvature, the time lag actually decreases. This is shown graphically in Figure 2 where a mixed signal of 50% velocity and 50% acceleration is compared temporally to velocity during a spiral drawing task adhering to the $^2/_3$ power law.

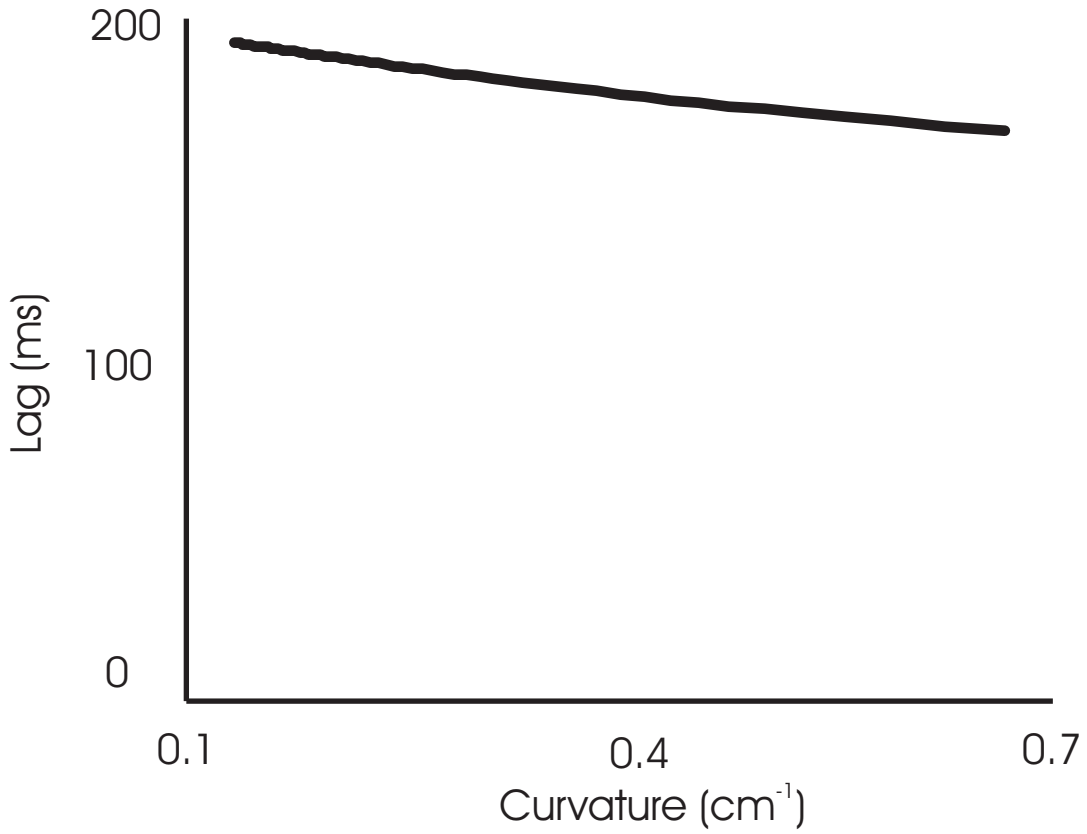

Figure 1: Effects of acceleration on M1 population vector lags as a function of curvature. Even though acceleration increases under higher curvature, the time lag of a PV sensitive to both acceleration and velocity decreases. Based on equation in Figure 4 caption of Todorov's paper without the stiffness term.

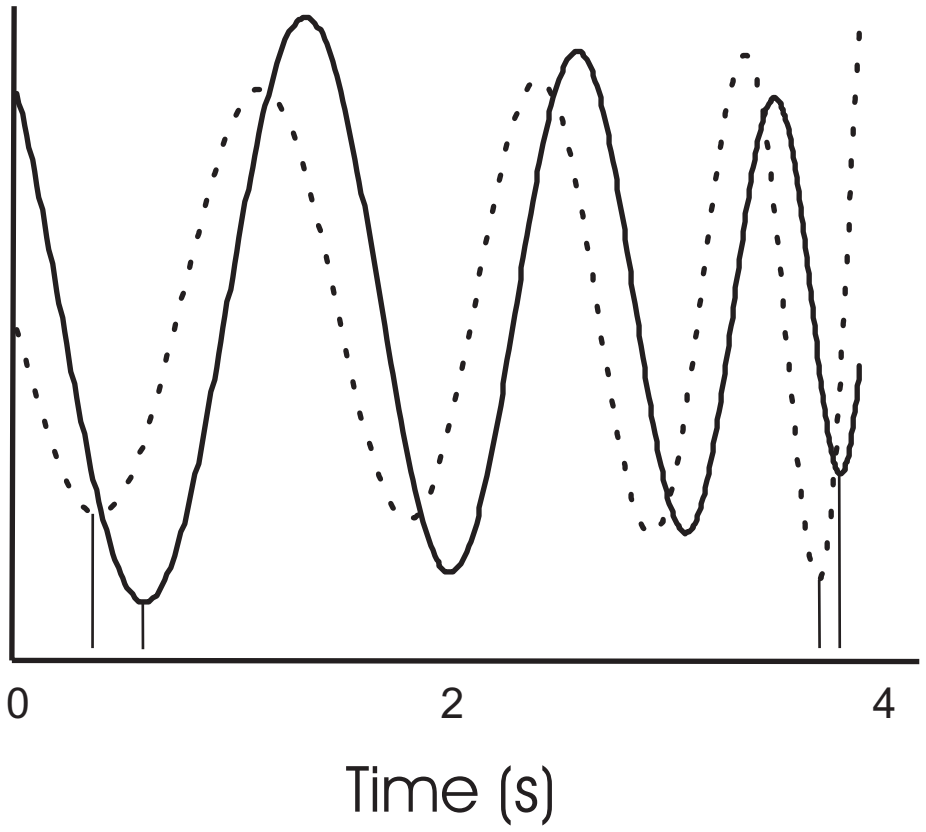

Figure 2: Temporal comparison of a simulated motor cortical cell and hand velocity during an outside->in spiral drawing task. The cell's activity (dotted line) is modulated by 50% velocity and 50% acceleration information. The second line (solid) represents the hand velocity signal (the component aligned with the cell's preferred direction). As the task progresses from the outside of the spiral inward toward higher curvatures, the cortical activity behaves more like the acceleration signal; however, since the angular velocity is also increasing, the time lag between cortical activity and velocity (thin lines) actually decreases.

Supplementary information for Apostolos P. Georgopoulos and James Ashe
Brain Sciences Center, Veterans Affairs Medical Center and Department of Neuroscience, University of Minnesota Medical School, Minneapolis, Minnesota 55417,USA
email: (A.P.G.): omega@tc.umn.edu

Table 1. Percentages of cells for which the noted variable yielded the highest R^2.

Variable	Motor cortex (N = 290)	
	Original analysis (from Table 1 in ref. 3)	New analysis
	Square-root transformed	Non-transformed
Target direction	46.55	42.76
Velocity	39.66	40.00
Position	7.24	8.97
Acceleration	6.55	8.27

Supplementary information for Emanuel Todorov

Gatsby Computational Neuroscience Unit, University College London, 17 Queen Square London WC1N 3 AR, UK
email: emo@gatsby.ucl.ac.uk

Response to Moran and Schwartz

Figure Legend:

Muscle force is $F(M,L,V) = (\text{af fl fv} + \text{f}_{\text{PE1}} + \text{af f}_{\text{PE2}})\, F_{\max}$, where muscle length L, velocity V, and stimulation frequency M are in dimensionless units[12], $F_{\max}$ is maximum potentiated force in endpoint space. The functions $\text{af}(M,L)$, $\text{fl}(L)$, $\text{fv}(L,V)$, $\text{f}_{\text{PE1}}(L)$, $\text{f}_{\text{PE2}}(L)$ with all 19 parameters defining them are described elsewhere[12]. The simpler form of the activation-frequency function $\text{af}(M,L)$ was used. All parameters were set to the average values for slow-twitch and fast-twitch muscles[12]. The plot in A) shows the surface $F(M,L,V)$ for M set to 1 (cyan), 0.5 (magenta), and 1.5 (yellow). Note that stiffness and damping (the partial derivatives with respect to Length and Velocity) are both determined by M and cannot be controlled independently.

The hand was modeled as a m = 1 kg point mass in 2-dimensional endpoint space, pulled by N muscles with uniformly distributed (unit) force directions $\mathbf{u}_{1\ldots N}$. With the new muscle model, stiffness and damping could no longer be set explicitly—instead they depended on the cocontraction level. Also, the PV could no longer be computed independent of tuning—so a concrete tuning function (cosine) was used. Given hand kinematics (1.5cm–7.5cm spiral traced in 2.5 seconds according to the 2/3 power law[2,3]), the PV at each point in time was computed in 5 steps:

1) Net force was $\mathbf{f} = m\ddot{\mathbf{x}}$.

2) Lengths L_i and velocities V_i were[1] $L_i = r_i - S\mathbf{x}^T\mathbf{u}_i$ and $V_i = -S\dot{\mathbf{x}}^T\mathbf{u}_i$. The scaling constant $S = 0.006$ mapped a 100cm range of motion in $\mathbf{x}$ to a 0.7–1.3 physiological range of normalized lengths L, and $r_{1\ldots N}$ defined the muscle lengths at the center $\mathbf{x} = \mathbf{0}$ of the workspace.

3) The individual force contribution F_i of each muscle was determined from the cosine tuning function $F_i = \frac{2}{N}\lfloor C + \mathbf{f}^T\mathbf{u}_i \rfloor$.

4) Stimulation frequencies M_i were found by solving $F_i = F(M_i, L_i, V_i)$.

5) The population vector $\sum (M_i - \overline{M}_i)\mathbf{u}_i$ was formed, with baselines $\overline{M}_i$ corresponding to maintained posture.

For nominal parameters $N = 10$, $F_{\max} = 30\,\mathrm{N}$, cocontraction was adjusted to $C = 15$ so that empirical stiffness K = 76 N/m and damping B = 9 Ns/m (found via perturbation experiments in the model) were close to the previously[1] used values of K = 50 N/m and B = 10 Ns/m. Results for 6 different parameter sets are shown, each averaged over 10 simulation runs with random $r_{1\ldots N}$ in the interval 0.9–1.1. The legend shows which parameter was varied from its nominal value (with resulting stiffness and damping). For all parameter settings, the timelag-curvature function closely resembled the original result[1] as well as the experimental data[2,3]. When gravity compensation was added to $\mathbf{f}$, the function fluctuated near the nominal curve. Similar fluctuations are present in experimental data[2,3], although the latter could be due to noise.

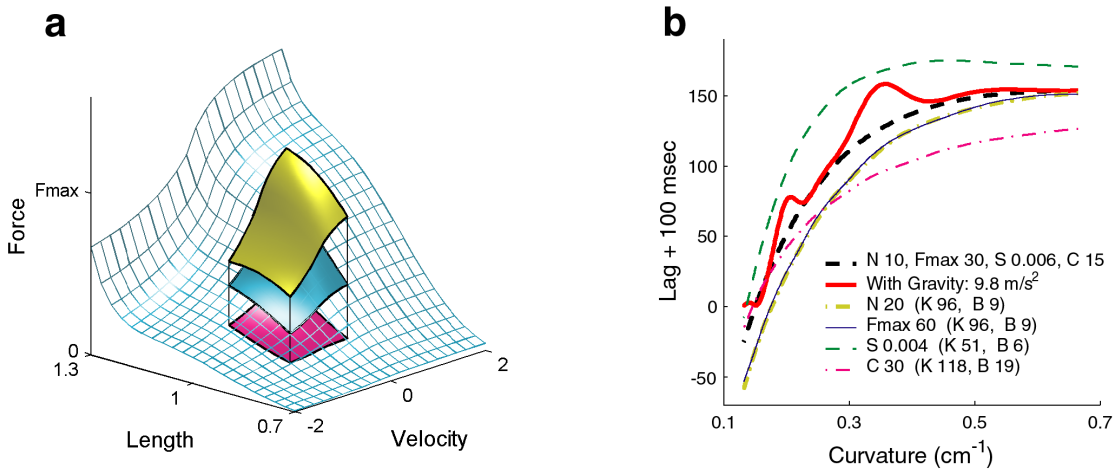

Response to Georgopoulos and Ashe:

Figure legend:

The plot visualizes the parameter space of synthetic response profiles. As before[1], synthetic mean firing rates at time t and angle q away from the preferred direction are $\mathrm{mfr}(t,q) = C + M\dot{x}(t)\cos(q) + 2B\lfloor \dot{x}(t)\cos(q) \rfloor + Kx(t)\cos(q)$, where C, M, B, K are sampled uniformly from 0–34, 0–4, 0–40, 0–200. Both the correct classification (the term with maximal absolute contribution) and the R^2 procedure applied to mfr are scale and translation invariant—so a two parameter plot $(B/M, K/M)$ can be obtained by subtracting C and dividing by M. The classification regions in the figure are computed through extensive simulations. Thin lines correspond to correct classification; thick lines - R^2 procedure applied to mfr; dotted lines - probability contours of classifying a cell as directional, R^2 procedure applied to raw binned spike trains; dashed lines - correct classification, two times faster movement. Line colors: red - position; green - velocity; blue - acceleration; black - direction. Color intensity corresponds to the 'confidence' of the correct classification, defined as the difference between the maximum and next

largest contribution. Spike train classification generally depends on all four parameters C, M, B, K, and is probabilistic because the same cell can be classified differently if a new set of Poisson spike trains are sampled. So the deterministic classification regions become probability distributions (dotted lines show the p = 0.5 and p = 0.3 contours of the probability of misclassifying cells as directional). When the same reaching movement is executed two times faster, hand displacement remains unchanged, velocity doubles, and acceleration quadruples - so the correct classification regions (dashed lines) change. The inset shows the response in the center of the region misclassified as directional. Note that this response does not look directional—it just does not fit in any of the alternative categories.

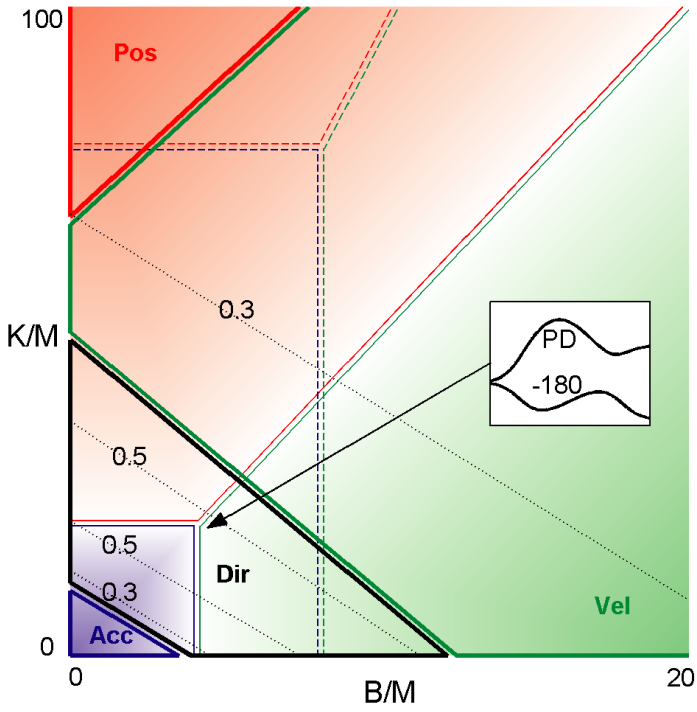

Acknowledgements:

I thank Paul Cisek, Zoubin Ghahramani, John Kalaska, and Stephen Scott for their suggestions to both responses.